On the temperature dependence of the current conduction mode in non-homogeneous Pt/n-GaN Schottky barrier diode

Mohammed Mamor, Khalid Bouziane, Hind Chakir, Pierre Ruterana

On the temperature dependence of the current conduction mode in non-homogeneous Pt/*n*-GaN Schottky barrier diode

Mohammed Mamor[1,3], Khalid Bouziane[2], Hind Chakir[1,2] and Pierre Ruterana[3]

[1]Laboratoire Physique Fondamentale et Appliquée–Safi (LPFA-Safi), Faculté Poly-Disciplinaire, B. P. 4162 Safi, Université Cadi Ayyad, Marrakech, Morocco.

[2]LERMA, Collège Ingénierie et Architecture, Université Internationale de Rabat, Parc Technopoles Rabat-Shore, 11100 Sala El Jadida, Morocco

[3]CIMAP, UMR 6252, CNRS, ENSICAEN, Université de Caen-Normandie, CEA, 6 Boulevard du Maréchal Juin, 1400 Caen, France.

Abstract

Forward current-voltage (*I-V*) measurements of Pt/*n*-GaN Schottky barrier diode (SBD) are investigated in a wide temperature range (80-400 K). The temperature dependence of the effective Schottky barrier height (SBH) and ideality factor are analyzed on the basis of the thermionic emission (*TE*) model by considering a double Gaussian distribution (DGD) of SBH due to the presence of barrier height inhomogeneities at the Pt/*n*-GaN interface. In the high temperature (HT) region (200-400 K), Pt/*n*-GaN SBD exhibits nearly an ideal behavior according to the *TE* conduction mode. The obtained values of the homogeneous SBH $\overline{\Phi}_{0bn}$ = 1.33 eV and Richardson constant A^*_{HT} = 26.86 A.cm^{-2}.K^{-2} are very close to the theoretical values for *n*-type GaN. In the low temperature (LT) region (80-160 K), the corresponding deduced values $\overline{\Phi}_{0bn}$ = 0.94 eV and A^*_{LT} = 14.74 A.cm^{-2}.K^{-2} according to the *TE* mode deviate strongly from the ideal behavior. This deviation is further supported by the large ideality factor. Therefore, the tunneling current including thermionic field emission (*TFE*) largely dominates the conduction mode at low temperature, as evidenced in this work.

Keywords: Barrier height Inhomogeneities; Temperature dependence of Schottky barrier height; Conduction mode in Pt/*n*-GaN structure.

*) Electronic mail: mohammedmamor@yahoo.om; m.mamor@uca.ac.ma

I. INTRODUCTION

GaN and its related alloys have attracted much interest over the past decade due to their potential application in the field of semiconductor devices [1, 2]. For instance, GaN semiconductor has promising physical features for the development of GaN-based high power, high speed and high frequency electronic devices such as the field effect transistors (MESFETs) [1, 2], and high electron mobility transistors (HEMTs) [3-5]. Of course the most popular examples of GaN-based applications include blue and ultraviolet (UV) light-emitting diodes (LEDs) [6]. In particular, GaN-based Schottky barrier diodes (SBD) have been used as a component for the above electronic and optoelectronic devices. In this respect, high quality ohmic and Schottky contacts are required. Therefore, a deep understanding of the electrical characteristics of metal (M)/GaN contacts is of fundamental and technological importance for developing GaN based-devices [7-9]. To this end, several challenges should be addressed in order to have M/GaN devices characterized with high Schottky barrier height (SBH), an ideality factor (n) close to unity and a low reverse current. Effectively, the low Schottky barrier height induces excess current through M/GaN SBD in both forward and reverse characteristics that strongly affects the SBD performances. The thermionic emission (*TE*) model is usually used to extract the Schottky parameters (barrier height and ideality factor), using current-voltage (*I-V*) measurements. The extracted values often exhibit an abnormal temperature dependence. This is reflected by the increase of the barrier height and the decrease of the ideality factor with increasing temperature. This abnormal behavior has been analyzed on the basis of *TE* model by taking into account the presence of the barrier height inhomogeneities (*BH*i) located at the metal/semiconductor (M/Sc) interface [10-16]. Actually, several models have been developed to describe the *BH*i at M/Sc interface [17-19]. The model developed by Werner and Güttler [17] considers a Gaussian distribution (GD) of SBH with standard deviation (σ_s) around mean barrier height ($\overline{\Phi}_{Bn}$). In the latter model, the effective SBH is shown to be both temperature and bias dependent.

Besides the abnormal features observed in previous reports [12-16], a double Gaussian distribution (DGD) of a non homogeneous M/Sc Schottky contacts has also been seen. It is associated

with low (LT) and high (HT) temperature regimes. Among other important electrical parameters, Richardson constant (*A**) is found to be strongly affected by the presence of *BH*i. This is especially true for the Richardson constant at low temperature regime (A^*_{LT}). For instance, Huan et *al* [12] and Yildirim et *al* [14] have assumed the existence of DGD of the barrier heights in Pt/*n*-4H-SiC and Ni/*n*-GaN, respectively. In the low temperature region, the extracted Richardson constant($A^*_{LT} =$ 37.4 A.cm^{-2}K^{-2}) for Pt/*n*-4H-SiC is found to be much lower than the theoretical value (146 A.cm^{-2}K^{-2}) [20, 21], by contrast to the corresponding high temperature region value $A^*_{HT} = 148.5$ A.cm^{-2}K^{-2}[12]. Other work on Ni/*n*-GaN system [14] reports *A** values determined by taking into account a DGD of SBH in the temperature regions of 80-180 K and 200-400 K as 80 and 85 A.cm^{-2}K^{-2}, respectively. On the other hand, Kumar et *al* [15] have obtained for Ni/*n*-GaN *A** values as 48 A.cm^{-2}K^{-2}in 100-200 K range and 29.2 A.cm^{-2}K^{-2} in 200-380 K range. Reddy et *al* [22] investigated the electrical properties of Ru/Pt/n-GaN in the temperature region of 100-420 K. By assuming a DGD, they reported, $A^*_{LT} = 10.29$ A.cm^{-2}K^{-2} and $A^*_{HT} = 27.83$A.cm^{-2}K^{-2}. Furthermore, Iucolano et *al* [23] and Zhou et al [24] have performed measurements on Pt/*n*-GaN system at high temperature regime only (300-450K) and (298-473 K), respectively. They obtained a single GD associated with high temperature A^*_{HT}value of 25 and 35 A.cm^{-2}K^{-2}, respectively. The above mentioned results indicate clearly a strong discrepancy in the deduced values of *A**. It is worth to mention that Pt-GaN system shows a very good rectifying characteristics with *A** at HT close to the theoretical value (26.9 A.cm^{-2}K^{-2}) [25] which makes it an ideal candidate for exploring further this discrepancy in the reported results. A systematic investigation of the temperature dependence of the electrical characteristics of Pt/*n*-GaN SBD over a wide temperature range should enable exploring the conduction modes, especially associated with the observed abnormal feature in the low temperature regime.

In this work, the temperature dependent forward current-voltage (*I*-*V*) characteristics were used to analyze the *BH*i at Pt/*n*-GaN SBD. In particular, the values of A^*_{LT} and A^*_{HT} deduced from the DGD of the barrier height are discussed in terms of current conduction modes at Pt/*n*-GaN SBD.

I. EXPERIMENTAL DETAILS

n-type GaN epitaxial layers with a free carrier density of (2–3)×10^{17} cm^{-3} and a thickness of about 1200 nm, was grown on (0001) Al_2O_3*c*-plane substrate using the metal organic chemical vapor deposition (MOCVD)growth technique. A low resistance ohmic contact was formed prior SBD fabrication by electron beam deposition of Ti/Al/Ni/Au on the front side of the GaN epilayer, and subsequent annealing at 500 ◦C for 5 min in a high purity Ar atmosphere [12]. Prior to Schottky contact deposition, the samples were degreased and dipped in an HCl:H2O (1:1) solution. Circular Pt Schottky contacts 0.66 mm in diameter and 120 nm in thickness were fabricated on the *n*-GaN epitaxial layers through a metal contact mask, by electron beam deposition.

Temperature-dependent *I –V* measurements on Pt/*n*-GaN SBDs were carried out in the range 80–400 K. The details of the SBD fabrication and *I-V* measurement have been reported elsewhere [16].

III. EXPERIMENTALRESULTS AND DISCUSSION

A. Investigation of electrical parameters based on thermionic emission conduction model.

Figure 1 displays the semi-logarithmic plot of the forward current –voltage measurements of Pt/*n*-GaN SBD as a function of temperature between 80 and 400 K. It shows that the forward ln (*I*)-*V* curve exhibits a linear behavior over a large applied forward voltage range for the considered temperature region. Moreover, the current increases with increasing temperature as predicted by the thermionic emission model regardless of the applied voltage considered.

In the framework of thermionic emission, the current through a SBD can be expressed as [26]:

$$I = I_s\left[\exp\left(\frac{q(V - R_s I}{nk_B T}\right) - 1\right] \tag{1a}$$

where *n is* the ideality factor, R_s the series resistance, V_F the applied forward voltage and I_s is the saturation current given by:

$$I_S = A^* S T^2 \exp(-\frac{\Phi_{0bn}}{k_B T}) \tag{1b}$$

Φ_{0bn} is the effective barrier height at zero bias, A^* the modified Richardson constant with a corresponding theoretical value of 26.9 A.cm^{-2}.K^{-2} for M/*n*-type GaN Schottky contacts [25], *S* the area of the diode, *T* the temperature and k_B the Boltzmann constant. The series resistance R_s was determined using the Werner method [27], while the ideality factor, *n* as defined in equation (1) was deduced from the slope of the semi logarithmic *I-V* characteristics.

$$n = \frac{q}{k_B T}\frac{dV}{d(\ln I)} \tag{2}$$

The respective experimental values of Φ_{0bn} and *n* were obtained from equations 1 and 2, and their temperature dependence is displayed in figure 2. The two Schottky parameters, Φ_{0bn} and *n* exhibit strong temperature dependence, namely Φ_{0bn} increases and *n* decreases with increasing temperature. This abnormal temperature dependence of Φ_{0bn} and *n* is usually interpreted in terms of barrier height inhomogeneities located at the M/Sc interface (12-16, 28-33].

According to the *BH*i model, the spatial inhomogeneities of SBH at the interface are interpreted in terms of a Gaussian spatial distribution of SBHs around zero-bias of mean value $\overline{\Phi}_{0bn}$ and with a zero-bias standard deviation σ_{0s} [13-16]. The measured effective barrier height (Φ_{0bn}) as a function of temperature is expressed:

$$\Phi_{0bn} = \overline{\Phi}_{0bn} - \frac{q^2\sigma_{0s}^2}{2k_B T} \tag{3}$$

The plot of Φ_{0bn} versus $1/2k_BT$ should then result in a straight line with a y-axis intercept equal to $\overline{\Phi}_{0bn}$ and a slope giving the zero-bias standard deviation σ_{0s}. The corresponding plot displayed in Fig. 3 shows a linear behavior but with two different slopes and also two different y-intercepts, with a transition occurring at 160 K. This result may indicate the presence of two Gaussian distributions of SBHs over the Schottky contact area. Accordingly, the deduced values at LT (80-160K) and HT (200-400 K) regions of the SBH zero-bias mean value $\overline{\Phi}_{0bn}$ and the associated zero-bias standard deviation σ_{0s} are ($\overline{\Phi}_{0bn}$ = 1.32 eV σ_{0s} = 140 mV) and ($\overline{\Phi}_{0bn}$ = 0.96 eV σ_{0s} = 86 mV), respectively.

The DGD assumption is supported by the fitting of Φ_{0bn} (T) shown in Fig. 2 using the above values of $\overline{\Phi}_{0bn}$ and σ_{0s}, where the two LT and HT temperature regions are clearly evidenced.

The presence of SBH inhomogeneity was also used to explain the deviation from linearity at low temperature in the conventional Richardson plot, namely ln (I_s/T^2) vs. $1/k_BT$. Considering the SBH inhomogeneity with double GD of the barrier heights, the modified Richardson plot can be obtained by combining equations (1b) and (3):

$$\ln\left(\frac{I_S}{T^2}\right)-\left(\frac{q^2\sigma_{0s}^2}{2k_B^2T^2}\right)=\ln\left(A^*S\right)-\frac{\overline{\Phi}_{0bn}}{2k_BT} \qquad (4)$$

The modified Richardson plots were determined using the two values of σ_{0s} corresponding to the HT and LT regions.

According to equation (4), the modified $\ln\left(\frac{I_S}{T^2}\right)-\left(\frac{q^2\sigma_{0S}^2}{2k_B^2T^2}\right)$ vs. $1/2k_BT$ plot (see Fig. 4) should be a straight line with the intercept at the ordinate giving the modified Richardson constant A^*, and the slope giving the zero-bias mean value of SBH, $\overline{\Phi}_{0bn}$. The solid squares represent the values corresponding to LT region calculated using σ_{0s} = 140 mV, and the open squares represent the values related to HT region calculated using σ_{0s} = 86mV. The result obtained from the analysis of the plots in Fig. 4 provides two sets of deduced values of A^* and $\overline{\Phi}_{0bn}$ corresponding to LT and HT regions (see Table I). The deduced $\overline{\Phi}_{0bn}$ values of 0.94 and 1.33 eV in the two temperature regions match well with the obtained values from the Φ_{0bn} vs. $1/2k_BT$ plots of Fig 3 (see Table I). While the extracted values of Richardson constant at HT region is found to be A^*_{HT} = 26.86 A.cm^{-2}.K^{-2}, in very good agreement with the theoretical value of 26.9 A.cm^{-2}.K^{-2}, its value A^*_{LT} = 14.74 A.cm^{-2}.K^{-2} at LT region is much lower.

This discrepancy between the theoretical value of A^* and the experimental extracted value in the low temperature range may indicate that the *TE* is not the major driving conduction mode. We argue that other modes of conduction such as the tunneling current including thermionic field emission (*TFE*) may principally govern the current transport at low temperature regime.

B. Investigation of the conduction modes in Pt/*n*-GaN SBD upon temperature.

The *BH*i model associated with Gaussian distribution of SBH shows however two distinct temperature regions. Current transport mode in each region (LT and HT) must therefore be considered in the evaluation of inhomogeneities at Pt/*n*-GaN contacts. The high temperature region presents often a behavior in accordance with thermionic conduction mode. In the low temperature region, the *I-V* characteristics could be characterized by a relatively excess of a forward current. This can be attributed to the presence of other dominant current transport modes such as quantum tunneling including thermionic field emission (*TFE*). Indeed, the values of the ideality factor much larger than the unity, the low values of both the barrier height and the Richardson constant obtained in the low temperature range (≤ 160 K) are usually an indication that the *TE* might no longer be the major conduction mode.

Considering the above abnormal features at low temperature regime, we suggest that the *TFE* is the dominant conduction mode as will be evidenced below. From now onwards, the focus will be on the results obtained in the low temperature range (≤ 160 K).

The *I-V* relation for a Schottky diode based on the *TFE* theory is given by [33]:

$$I = I_s\left[\exp\left(\frac{q(V - R_s I}{E_0}\right) - 1\right] \tag{5a}$$

where

$$I_{s,TFE} = SA^*T\frac{\sqrt{\pi qE_{00}(\Phi_{bnt}-V)-(E_C-E_F)}}{k_B\cosh(\frac{E_{00}}{k_BT})}\ exp\left[-\frac{E_C-E_F}{k_BT}\right]exp\left[\frac{(E_C-E_F)+q(V-\Phi_{bnt})}{E_0}\right] \tag{5b}$$

with $E_0 = E_{00}\coth\left[\frac{E_{00}}{k_BT}\right] = n_{tun}k_BT$

In Eq. (5b), E_{00} corresponds $E_{00} = \hbar/2\left[\frac{N_D}{m^*\varepsilon_s}\right]^{1/2}$

where N_D is the doping density, m^* the effective mass of electron, and ε_s the dielectric constant of GaN.

The depth of Fermi level below the conduction band minimum E_C is expressed as:

$$E_C - E_F = k_B T \ln(\frac{N_C}{N_D}) \quad (6)$$

where N_C is the effective density of states in the conduction band expressed at given temperature T by:

$$N_C(T) = \frac{2}{h^3}(2\pi m_e^* k_B T)^{\frac{3}{2}} = 2.5\times10^{19}\left[\frac{m^*}{m_0}\right]^{\frac{3}{2}}\left[\frac{T}{T_0}\right]^{\frac{3}{2}} \quad (7)$$

where T_0 is the room temperature, m_0 is the free electron mass; the other constants have their usual meaning.

The doping density N_D obtained from *C-V* measurement for this GaN sample of about 3×10^{17} cm^{-3} is weakly temperature dependent, whereas N_C decreases substantially with decreasing temperature. The variation of both N_C and (E_C-E_F) as a function of temperature is shown in Fig. 5. The Fermi level lies in the vicinity of the conduction band at lower temperature, with a maximum value of 14.7 meV at 160 K. Therefore, this GaN can be considered as a degenerate semiconductor likewise heavily doped. This result supports further the assumption that the current transport mode across SBD is dominated by the quantum tunneling transport [34]. Indeed, the *I-V-T* curves at temperature below 160 K are well fitted using Eqs. (5a) and (5b) based on the *TFE* model as shown in Fig. 6. The extracted characteristics parameters from fitting curves using Eqs. (5a) and (5b), namely n_{tun}, Φ_{bnt}, and E_C-E_F based on *TFE* model are reported in Table II.

The above results provide a good evidence that the existence of the DGD, usually observed in M/Sc contacts can be well interpreted in terms of two different conduction modes: (i) a dominant thermionic emission mode at high temperature regime, and (ii) a dominant tunneling thermionic field emission at low temperature regime.

IV. CONCLUSION

In this work, we have investigated the temperature dependence of the forward current-voltage characteristics of Pt/*n*-GaN Schottky contacts in order to explain the abnormal behavior usually observed associated with the double Gaussian distribution of the SBH within the *TE* model. The DGD is associated with two main regions, usually low (80-160K) and high (200-400) temperature range.

Numerous works show incoherent values of SBH, ideality factor and Richardson constant at low temperature region. We show in this work that the above abnormal features observed at low temperature is correlated with the use of the *TE* conduction mode. In this work, the *TFE* model has been utilized to interpret properly the low temperature regime. The deviation from the *TE* current at low temperature is thus explained by the occurrence of close degeneracy of GaN and the whole *I-V* characteristics at low temperature region are well fitted within the *TFE* model.

Therefore, it is important to consider tunneling conduction mode at low temperature regime when investigating the barrier height inhomogeneities in devices involving GaN-based Schottky contacts.

REFERENCES

[1] K.J. Chen, O. Häberlen, A. Lidow, C.L. Tsai, T. Ueda, Y. Uemoto and Y. Wu, GaN-on-Si Power Technology: Devices and Applications, IEEE Trans. Electron Devices. **64**, 779 (2017).

[2] S. Singh, T. Chaudhary and G. Khanna, Recent Advancements in Wide Band Semiconductors (SiC and GaN) Technology for Future Devices, *Silicon* **14**, 5793 (2022).

[3] C. Lee, W. Lin, Y. Lee, and J. Huang, Characterizations of Enhancement-Mode Double Heterostructure GaN HEMTs With Gate Field Plates, IEEE Trans. Electron Devices. **65**, 488 (2018).

[4] S. J. Pearton and F. Ren, GaN Electronics, Advanced Materials. **12,** 1571 (2000).

[5] T. H Yang, J. Brown, K. Fu, J. Zhou, K. Hatch, C. Yang, J. Montes, X. Qi, H. Fu, R. J. Nemanich, and Y. Zhao, AlGaN/GaN metal–insulator–semiconductor high electron mobility transistors (MISHEMTs) using plasma deposited BN as gate dielectric, Appl. Phys. Lett. **118**, 072102 (2021).

[6] S. Nakamura and G. Fasol, The blue laser diode, (Springer Verlag, 1997).

[7] N. K. R. Nallabala, S. Godavarthi, V. K. Kummara, M. K. Kesarla, D. Saha, H. S. Akkera, G. K. Guntupalli, S. Kumar, S. V. P. Vattikuti, Structural, optical and photo response characteristics of metal-insulator-semiconductor (MIS) type Au/Ni/CeO_2/GaN Schottky barrier ultraviolet photodetector, Materials Science in Semiconductor Processing. **117**, 105190 (2020).

[8] B. Shankar, A. Soni and M. Shrivastava, Electro-Thermo-Mechanical Reliability of Recessed Barrier AlGaN/GaN Schottky Diodes Under Pulse Switching Conditions, in IEEE Trans. Electron Devices. **67**, 2044 (2020).

[9] J. Koba and J. Koike, Low contact resistivity of metal/n-GaN by the reduction of gap states with an epitaxially grown GaO_x insulating layer, AIP Advances, **12**, 085302 (2022).

[10] L. Huang, F. Qin, S. Li and D. Wang, Effects of surface properties on barrier height and barrier inhomogeneities of platinum contacts to n-type 4H-SiC, Appl. Phys. Lett. **103**, 033520 (2013).

[11] S. Shivaraman, L. H. Herman, F. Rana, J. Park, and M. G. Spencer, Schottky barrier inhomogeneities at the interface of few layer epitaxial graphene and silicon carbide, Appl. Phys. Lett. **100**, 183112 (2012).

[12] L. Huang and D. Wang, Barrier inhomogeneities and electronic transport of Pt contacts to relatively highly doped n-type 4H SiC, J. Appl. Phys. **117**, 204503 (2015).

[13] F. M. Coşkun, O. Polat, M. Coşkun, A. Turut, M. Caglar, Z. Durmus, and H. Efeoğlu, Temperature dependent current transport mechanism in osmium-doped perovskite yttrium manganite-based heterojunctions, J. Appl. Phys. **125**, 214104 (2019).

[14] N. Yıldırım, K. Ejderha and A. Turut, On the temperature-dependent experimental I-V and C-V data of Ni/n-GaN Schottky contacts, J. Appl. Phys. **108**, 114506 (2010).

[15] A. Kumar, S. Vinayak and R. Singh, Micro-structural and temperature dependent electrical characterization of Ni/GaN Schottky barrier diodes, Current Applied Physics. **13**, 1137 (2013).

[16] M. Mamor, Interface gap states and Schottky barrier inhomogeneity at metal/*n*-type GaN Schottky contacts, J. Phys.: Condens. Matter. **21**, 335802 (2009).

[17] J. H. Werner and H. H. Güttler, Barrier inhomogeneities at Schottky contacts, J. Appl. Phys. **69**, 1522 (1991).

[18] R. T. Tung, Electron transport at metal-semiconductor interfaces: General theory, Phys. Rev. B. **45**, 13509 (1992).

[19] P. Song, R. L. Van Meirhaeghe, W. H. Laflere, and F. Cardon, On the difference in apparent barrier height as obtained from capacitance-voltage and current-voltage-temperature measurements on Al/*p*-InP Schottky barriers, Solid State Electron. **29**, 633 (1986).

[20] A. Itoh, T. Kimoto, and H. Matsunami, High performance of high-voltage 4H-SiC Schottky barrier diodes, IEEE Trans. Electron Devices. **16**, 280 (1995).

[21] F. Roccaforte, F. L. Via, V.Rainer, R. Pierobon and E. Zanoni, Richardson's constant in inhomogeneous silicon carbide Schottky contacts, J. Appl. Phys. **93**, 9137 (2003).

[22] N.N. K. Reddy and V. Reddy, Barrier characteristics of Pt/Ru Schottky contacts on *n*-type GaN based on *I–V–T* and *C–V–T* measurements, Bull. Mater. Sci, **35**, 53 (2012).

[23] F. Iucolano, F. Roccaforte, F. Giannazzo, and V. Raineri, Barrier inhomogeneity and electrical properties of Pt/GaN Schottky contacts, J. Appl. Phys. **102**, 113701 (2007).

[24] Y. Zhou, D. Wang, C. Ahyi, C.-C. Tin, J. Williams, M. Park, N. M. Williams, A. Hanser, and E. A. Preble, Temperature-dependent electrical characteristics of bulk GaN Schottky rectifier, J. Appl. Phys. **101**, 024506 (2007).

[25] A. M. Witowski, K. Pakuła, J. M. Baranowski, M. L. Sadowski, and P. Wyder, Electron effective mass in hexagonal GaN, Appl. Phys. Lett. **75**, 4154 (1999). https://doi.org/10.1063/1.125567.

[26] E. H. Rhoderick and R. H. Williams, *Metal-Semiconductor Contacts*, 2nd ed. Clarendon Press, Oxford, UK: Oxford Science, (1988), p. 38.

[27] J. H. Werner, Schottky barrier and pn-junction *I/V* plots — Small signal evaluation, *Appl. Phys.* A. **47,** 291 (1988).

[28] M. Mamor, K. Bouziane and A. Tirbiyine, Barrier inhomogeneities in titanium Schottky contacts formed on argon plasma etched p-type $Si_{0.95}Ge_{0.05,}$ J. Mater. Sci: Mater Electron. **25**, 1527 (2014).

[29] N. Yıldırım, A. Turut, and V. Turut, The theoretical and experimental study on double-Gaussian distribution in inhomogeneous barrier-height Schottky contacts, Microelectron. Eng. **87**, 2225 (2010).

[30] S. Chand and S. Bala, Analysis of current–voltage characteristics of inhomogeneous Schottky diodes at low temperatures, Appl. Surf. Sci. **252**, 358 (2005).

[31] M. Mamor, K. Bouziane, A. Tirbitine and H. Alhamrashdi, On the electrical characteristics of Au/*n*-type GaAs Schottky diode, Superlattices and Microstructures. **72**, 344 (2014).

[32] N. Yıldırım and A. Turut, A theoretical analysis together with experimental data of inhomogeneous Schottky barrier diodes, Microelectron. Eng. **86**, 2270 (2009).

[33] F. H. Padovani and R. Stratton, Field and thermionic-field emission in Schottky barriers, Solid-State Electron. **9**, 695 (1966).

[34] D. K. Schroder, Semiconductor Material and Device Characterization, Wiley Interscience, Hoboken, NJ, 2006, p.160.

“Data Availability Statement”

The datasets generated during and/or analyzed during the current study are available from the corresponding author on reasonable request.

FIGURE CAPTIONS

Fig. 1. (Color online) Experimental forward *I–V* curves of Pt/*n*-GaN measured at different temperatures.

Fig. 2. Deduced **e**ffective barrier heights, Φ_{0bn} and ideality factor, *n* as a function of temperature for Pt/*n*-GaN. Broken and solid lines are for the calculated SBHs using equation (3) for two Gaussian distributions of SBHs in LT region (80-160 K) and HT region (200-400 K), respectively.

Fig. 3. (Color online) The effective barrier heights Φ_{0bn} vs. $1/2k_BT$ curves of Pt/*n*-GaN SBD according to the barrier inhomogeneous model [17].

Fig. 4. (Color online) Modified Richardson plots $\ln\left(\frac{I_s}{T^2}\right)-\left(\frac{q^2\sigma_{0S}^2}{2k_B^2T^2}\right)$ vs. $(1/k_BT)$ associated with both LT and HT regions.

Fig. 5. Effective density of states N_C and the energy difference between the conduction band minimum and Fermi level (E_C-E_F) of Pt/*n*-GaN SBD as a function of temperature.

Fig. 6. Experimental forward current curve at the temperatures of 80, 120, and 160 K, and the corresponding fitting curves to *I-V* characteristics according to the *TFE* model.

Table I. Summary of the extracted experimental homogenous SBH and Richardson's constant in the LT and HT regions, along with the results reported in the literature.

System	Theoretical A.cm^{-2}.K^{-2}	A^*_{LT} A.cm^{-2}.K^{-2}	A^*_{HT} A.cm^{-2}.K^{-2}	$\overline{\Phi}_{0bn}$ (eV) (LT)	$\overline{\Phi}_{0bn}$ (eV) (HT)	References
Pt/*n*-GaN	26.9	14.74	26.86	0.94	1.33	This work
Ru/Pt/n-GaN		10.29	27.83	0.47	0.99	[22]
Pt/*n*-GaN		NA	25	NA	1.21	[23]
Pt/*n*-GaN		NA	35	-	-	[24]
Ni/*n*-GaN		80	85	0.72	1.42	[14]
Ni/*n*-GaN		48	29.2	0.73	1.4	[15]

(NA) Not Applicable. *I-V* measurements have been have performed on M/*Sc* system at high temperature regime only.

Table II. Summary of the fitting parameters used for *I-V* characteristics of Pt/*n*-GaN in *TFE* mode.

Temperature (K)	Φ_{bnt} (eV)	n_{tun}	E_C-E_F (meV)
80	1.01	1.38	0.18
120	1.04	1.17	6.56
160	1.06	1.01	14.70

Fig. 1/6

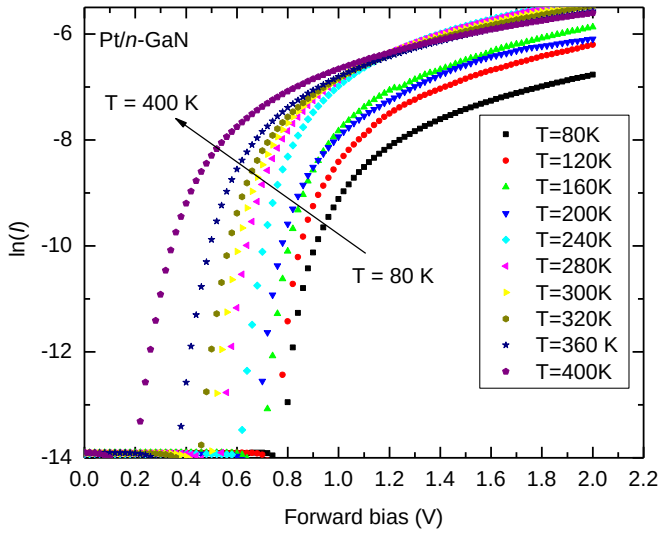
Pt/n-GaN
T = 400 K
T = 80 K
T=80K
T=120K
T=160K
T=200K
T=240K
T=280K
T=300K
T=320K
T=360 K
T=400K
ln(I)
Forward bias (V)
-6
-8
-10
-12
-14
0.0
0.2
0.4
0.6
0.8
1.0
1.2
1.4
1.6
1.8
2.0
2.2

Fig. 2/6

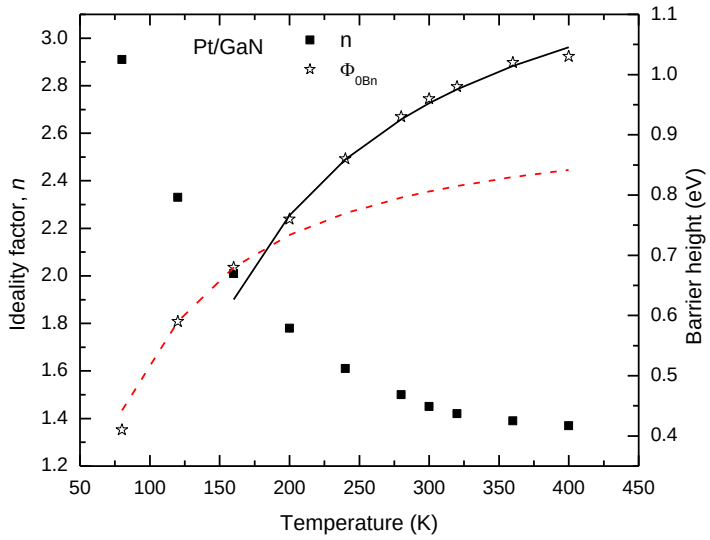
Pt/GaN
n
Φ_{0Bn}
Ideality factor, n
Barrier height (eV)
Temperature (K)
3.0
2.8
2.6
2.4
2.2
2.0
1.8
1.6
1.4
1.2
1.1
1.0
0.9
0.8
0.7
0.6
0.5
0.4
50
100
150
200
250
300
350
400
450

Fig. 3/6

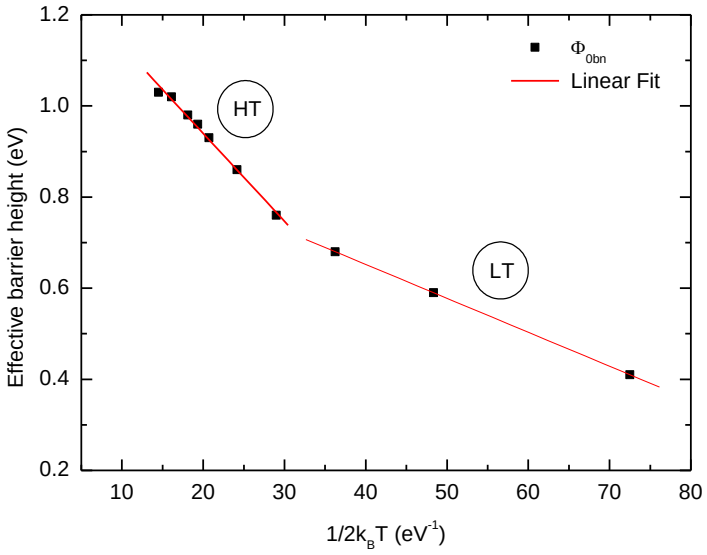
1.2
1.0
0.8
0.6
0.4
0.2
Effective barrier height (eV)
10
20
30
40
50
60
70
80
1/2k_BT (eV^-1)
Φ_0bn
Linear Fit
HT
LT

Fig. 4/6

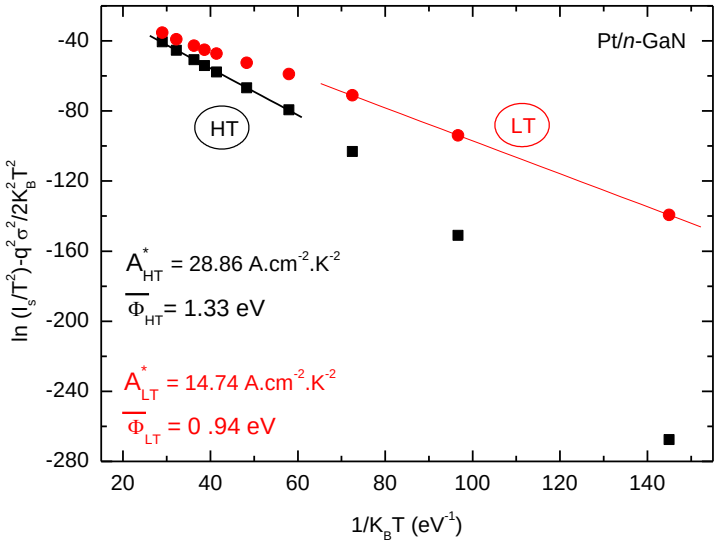
Pt/n-GaN
HT
LT
A*HT = 28.86 A.cm-2.K-2
ΦHT= 1.33 eV
A*LT = 14.74 A.cm-2.K-2
ΦLT = 0 .94 eV
ln (Is/T2)-q2σ2/2K2BT2
1/KBT (eV-1)
-40
-80
-120
-160
-200
-240
-280
20
40
60
80
100
120
140

Fig.5/6

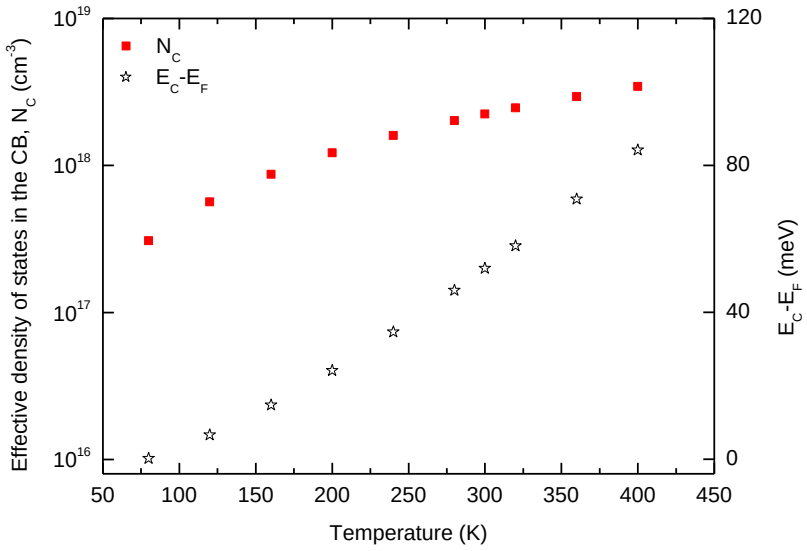
10^{19}
10^{18}
10^{17}
10^{16}
120
80
40
0
N_C
E_C-E_F
Effective density of states in the CB, N_C (cm^{-3})
E_C-E_F (meV)
50
100
150
200
250
300
350
400
450
Temperature (K)

Fig. 6/6

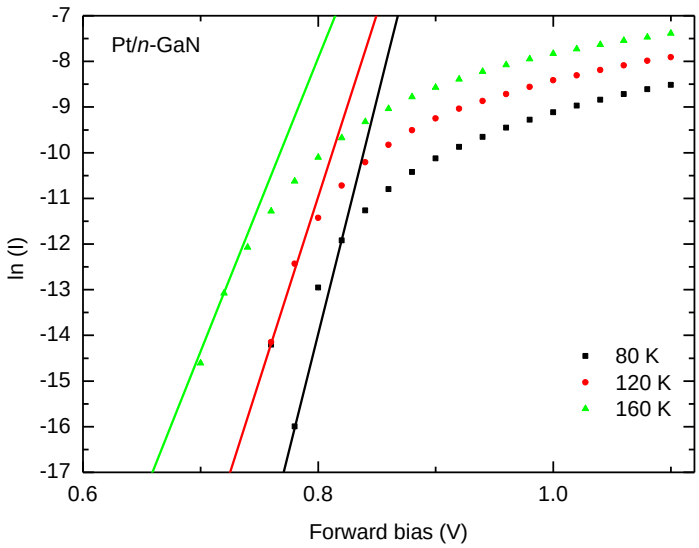
Pt/n-GaN
ln (I)
Forward bias (V)
80 K
120 K
160 K
-7
-8
-9
-10
-11
-12
-13
-14
-15
-16
-17
0.6
0.8
1.0